

Further Analysis of the 2-2 Wire-Driven Parallel Crane

Jean-Pierre Merlet

► **To cite this version:**

Jean-Pierre Merlet. Further Analysis of the 2-2 Wire-Driven Parallel Crane. Federico Thomas and Alba Perez Gracia. CK2013 - 6th Int. Workshop on Computational Kinematics, May 2013, Barcelone, Spain. 2013, Computational Kinematics. <10.1007/978-94-007-7214-4_2>. <hal-01211797>

HAL Id: hal-01211797

<https://hal.inria.fr/hal-01211797>

Submitted on 5 Oct 2015

HAL is a multi-disciplinary open access archive for the deposit and dissemination of scientific research documents, whether they are published or not. The documents may come from teaching and research institutions in France or abroad, or from public or private research centers.

L'archive ouverte pluridisciplinaire **HAL**, est destinée au dépôt et à la diffusion de documents scientifiques de niveau recherche, publiés ou non, émanant des établissements d'enseignement et de recherche français ou étrangers, des laboratoires publics ou privés.

Further analysis of the 2-2 wire-driven parallel crane

J-P. Merlet

Abstract The 2-2 wire-driven parallel crane is the most simple planar parallel crane actuated by wires with two wires connected at two different points on the platform. We present original contributions on the kinematics of such robot, namely full inverse kinematics, trajectory, static and singularity analysis in the joint space.

Key words: cable robot, kinematics

1 Introduction

The 2-2 wire-driven parallel crane has two coilable wires connected at two different points B_1, B_2 on the platform (figure 1). The wires can be coiled by winches fixed to the ground, whose output points are A_1, A_2 . Hence, provided that gravity is included, it is a 2 d.o.f. robot that allows to control the planar motion of the platform center of mass G , that lies in the vertical plane that includes A_1, A_2 (and also includes B_1, B_2). The lengths of the wires will be denoted by ρ_1, ρ_2 . We will assume that the distance between B_1, B_2 is smaller than the distance between A_1, A_2 so that both wires cannot be parallel. To the best of the author's knowledge the kinematics of such a robot has been addressed only in [3, 5].

We introduce a reference frame $\mathcal{R} = (A_1, \mathbf{x}, \mathbf{y})$ where \mathbf{y} is the vertical direction pointing upward. In this frame the coordinates of A_2 are $(x_{a_2} > 0, y_{a_2})$ and the coordinates of G are (x_g, y_g) . We also define a mobile frame $\mathcal{R}_m = (G, \mathbf{x}_m, \mathbf{y}_m)$ and in this frame the coordinates of the B_i are (x_{b_i}, y_{b_i}) .

A rotation matrix \mathbf{R} of angle θ is used to get the components in \mathcal{R} of a vector whose components is known in \mathcal{R}_m . Especially the coordinates (x_i, y_i) of B_i in \mathcal{R} are obtained as:

$$x_i = x_g + \cos \theta x_{b_i} - \sin \theta y_{b_i} \quad y_i = y_g + \sin \theta x_{b_i} + \cos \theta y_{b_i} \quad (1)$$

The length ρ_i of wire i is obtained as

$$\rho_i^2 = (x_i - x_{a_i})^2 + (y_i - y_i)^2 \quad (2)$$

J-P. Merlet, INRIA, e-mail: Jean-Pierre.Merlet@inria.fr

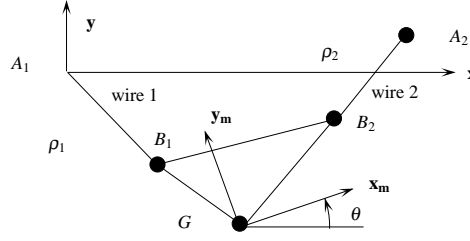


Fig. 1 The 2-2 robot

Let $\mathcal{F} = (0, -mg, 0, 0, 0, 0)^T$ be the force and torque applied on the platform, where m is its mass and let $\tau = (\tau_1, \tau_2)^T$ be vector of tensions in the wires. Static equilibrium is obtained when

$$\mathcal{F} = \mathbf{J}^{-T} \tau \quad (3)$$

where \mathbf{J}^{-T} is a 6×2 matrix whose i -th column \mathbf{J}^{-T}_i is

$$\mathbf{J}^{-T}_i = \left(\frac{\mathbf{A}_i \mathbf{B}_i}{\rho_i} \quad \frac{\mathbf{G} \mathbf{B}_i \times \mathbf{A}_i \mathbf{B}_i}{\rho_i} \right)^T \quad (4)$$

This column is the Plücker vector of the line going through A_i, B_i while \mathcal{F} is the vertical line going through G . Equation (3) indicates that at mechanical equilibrium the lines $A_1 B_1, A_2 B_2$ and the vertical line going through G span a linear complex i.e. meet at the same point. Note that the coordinate of $\mathbf{A}_i \mathbf{B}_i$ along the z axis of \mathcal{R} is 0 and consequently (3) admits a reduced form: if $\mathcal{F}_r = (0, -mg, 0)^T$ and \mathbf{J}^{-T}_r is a matrix whose i -th column is $\left(\frac{\mathbf{A}_i \mathbf{B}_{ix}}{\rho_i}, \frac{\mathbf{A}_i \mathbf{B}_{iy}}{\rho_i}, \frac{\mathbf{G} \mathbf{B}_{ix} \mathbf{A}_i \mathbf{B}_{iy} - \mathbf{G} \mathbf{B}_{iy} \mathbf{A}_i \mathbf{B}_{ix}}{\rho_i} \right)$, then we have

$$\mathcal{F}_r = \mathbf{J}^{-T}_r \tau \quad (5)$$

Let us define the 3×3 matrix \mathbf{M} whose first and third columns are the first and second columns of \mathbf{J}^{-T}_r , while its second column is \mathcal{F}_r . If we define $\alpha = (\tau_1, -1, \tau_2)$, then equation (5) may be written as $\mathbf{M} \alpha = \mathbf{0}$. As α is not equal to 0 the mechanical equilibrium condition may also be written as:

$$|\mathbf{M}| = 0 \quad (6)$$

Note that equations (5,6) are only necessary conditions for mechanical equilibrium as we have also to ensure that the tensions in the wires are all positive.

2 Trajectory, equilibrium condition and inverse kinematics

Let (X_i, Y_i) be the components of the vector $\mathbf{G} \mathbf{B}_i$ in \mathcal{R} . The equilibrium condition (6) may be written as

$$(Y_2 - Y_1)x_g^2 + (X_1 - X_2)x_g y_g + (x_{a_2}(Y_1 - Y_2) + y_{a_2}X_2 + Y_2X_1 - Y_1X_2)x_g - x_{a_2}X_1 y_g + X_1(y_{a_2}X_2 - x_{a_2}Y_2) = 0 \quad (7)$$

Hence if θ is fixed (and consequently so are the X_i, Y_i), then G moves along an hyperbola whose principal axes makes an angle ϕ with the \mathbf{x} axis (such that $\tan(2\phi) = (X_1 - X_2)/(Y_2 - Y_1)$) and whose center admits $x_{a_2}X_1/(X_1 - X_2)$ as x coordinate. An analysis of this hyperbola allows one to determine if a given orientation θ is reachable either over the full workspace or at least on part of it. For example the coefficient of y_g in (7) cancels for $x_g = x_g^s = x_{a_2}X_1/(X_1 - X_2)$; consequently if $x_g^s \in [0, x_{a_2}]$, then the workspace is separated into two components and it is not possible to maintain the given orientation over the workspace of the crane. Note that the equilibrium condition (7) is a function of x_g, y_g, θ but we will see in section 3 that it may also be expressed as a function of x_g, y_g, ρ_1, ρ_2 .

While the 2-2 is a 2 d.o.f. robot, the platform has still 3 d.o.f. Hence for solving the inverse kinematics it is necessary to specify 2 of this 3 d.o.f while the value of the remaining variable X will be determined by solving the equation (7). We examine now the possible different cases:

- x_g, θ are fixed: equation (7) is linear in y_g , there is a single possible value for y_g
- y_g, θ are fixed: equation (7) is a second order polynomial in x_g , there is up to two possible values for x_g
- x_g, y_g are fixed: using the Weierstrass substitution on (7) leads to a 4-th order polynomial in $T = \tan(\theta/2)$ that may have 4 real roots that furthermore leads to positive tensions in the wires. For example for $x_{a_2} = 20, y_{a_2} = 10, x_{b_1} = -20, x_{b_2} = 20, y_{b_1} = y_{b_2} = 1, x_g = 10, y_g = -20$ we get indeed 4 possible values for θ that all leads to positive wire tensions.

3 Direct kinematics

The direct kinematics (DK) of the 2-2 robot has been presented in [5]. The solutions can be obtained by solving a 12th order univariate polynomial and [5] provides a geometrical explanation of order of the polynomial that is related to the sextic nature of the coupler curve of the 2-2. But, as mentioned by Carricato [3] if the platform may perform out of the plane motion, then there may be up to 24 solutions: indeed we have to consider possible reflection of the problem or equivalently we have to consider the solutions that are obtained when reversing the role of A_1, A_2 .

We first simply propose here another approach to derive the 12th order polynomial. The static equilibrium condition (7) is a function of $\sin\theta, \cos\theta$, while equations (2) are linear functions of these quantities. Solving these 2 equations in these unknowns and reporting the result in (7) leads to an equilibrium condition \mathcal{E}_1 that is function of x_g, y_g, ρ_1, ρ_2 of degree 7 in x_g and 6 in y_g . The constraint $\sin^2\theta + \cos^2\theta - 1 = 0$ leads to another equation \mathcal{E}_2 . The resultant of $\mathcal{E}_1, \mathcal{E}_2$ in y_g is a 24th order polynomial in x_g that factors out in a 12th order polynomial and a 3rd order polynomial that is raised at the power of 4. This second polynomial provides

only solutions with $y_g > 0$ while the first polynomial provides the valid solutions. Stability analysis of these solutions have been addressed in [1],[2].

We have then to consider that obtaining all the solutions from the solving of the univariate polynomial may not be the best method: indeed numerical round-off errors will affect the calculation of the polynomial coefficients while the solving of a 12th order polynomial may be numerically unstable. Instead of using the polynomial, it is possible to transform the problem into an eigenvalue problem, which is numerically more stable, but still the results cannot be guaranteed. Hence we propose to use interval analysis (IA) on a set of DK equations, as this method allows to provide **all** solutions **exactly** (i.e. with an arbitrary accuracy). The efficiency of this method is however dependent upon the set of equations that has to be solved. Hence we may consider several forms of the problem:

1. with 8 equations and 8 unknowns: these unknowns are $x_g, y_g, x_1, y_1, x_2, y_2, \tau_1, \tau_2$. The equations are the 5 equations (2,3) and the 3 geometrical constraints \mathcal{G} defined as $\|\mathbf{B}_1\mathbf{B}_2\|^2 = d_{12}^2, \|\mathbf{B}_1\mathbf{G}\|^2 = d_{1G}, \|\mathbf{B}_2\mathbf{G}\|^2 = d_{2G}$, where d_{12}, d_{1G}, d_{2G} are the known distances between $(B_1, B_2), (B_1, G), (B_2, G)$
2. with 6 equations and the 6 unknowns $x_g, y_g, x_1, y_1, x_2, y_2$. The constraints are the 3 equations (2,6) and the 3 geometrical constraints \mathcal{G}
3. with 5 equations and the 5 unknowns $x_g, y_g, \theta, \tau_1, \tau_2$. The constraints are the 5 equations (2,3)
4. with 4 equations and the 4 unknowns $x_g, y_g, \sin \theta, \cos \theta$. The constraints are the 3 equations (2,6) and the constraint $\sin^2 \theta + \cos^2 \theta = 1$.
5. with 3 equations and the 3 unknowns x_g, y_g, θ . The constraints are the 3 equations (2,5).
6. with 2 equations and 2 unknowns: these unknowns are either x_g or y_g and θ . The difference between the two equations (2) is linear in x_g, y_g and is used to obtain one of these variables. The constraints are one of (2) and (5)

Note that methods 1 and 2 take reflection into account and hence provide all solutions in a single pass, while the other methods required to be applied twice.

To compare the efficiency of the solving in the various cases we consider a specific robot, called *test robot*, that will be used all over this paper, such that: $A_1 = (0, 0)$ $A_2 = (100, 10)$ $B_1 = (-10, 1)$ $B_2 = (10, 2)$ and we solve the DK for $\rho_1 = 110, \rho_2 = 100$. The solving times in seconds for the above methods are 0.95 (4), 0.49 (4), 0.8 (2), 0.04 (2), 0.11 (2), 3.66 (6), where the number in parenthesis is the number of solutions. The total number of solutions with positive tensions is 4 as indicated by methods 1 and 2. Methods 3, 4, 5 provide only half of the solutions because reflection is not taken into account and method 6 provides 6 solutions but only 2 with positive tensions. Hence the most efficient methods are 2 and 4 (which requires 2 passes to get all solutions).

We have conducted a study of the number of solutions with positive tensions by selecting randomly 400 wire lengths and solving the DK in each case. We have found that the DK has 2 solutions in 34% of the cases, 3 in 8.75%, 4 in 45.5% 5 in 0.75%, 6 in 8.5%, 7 in 0.5 % and 8 in 2%. Evidently we cannot claim that even with this relatively high number of trials these numbers will always be relevant. Figure 2

shows an example with 8 solutions obtained for $\rho_1 = 180, \rho_2 = 190$. The solution (x_g, y_g, θ) obtained for the rotation matrix are $(45.19, -168.50, 174.79)$, $(30.31, -168.47, 142.38)$, $(49.34, -177.12, 3.10)$, $(68.01, -168.40, 223.97)$ with θ in degree. For the reflection we get $(48.46, -171.49, 175.96)$, $(12.35, -169.36, 85.78)$, $(49.29, -174.13, 357.43)$, $(85.36, -169.37, 267.40)$. Note that if out of the plane motion is possible, then we have only 2 stable solutions.

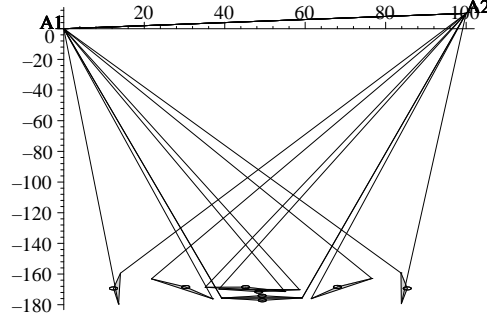


Fig. 2 The eight solutions of the DK obtained for the test robot with $\rho_1 = 180, \rho_2 = 190$

4 Statics in the joint space

If the pose parameters are known, then equations (3) allows to determine the tensions in the wires. It may however be of interest to study kinematics in the joint space ρ_1, ρ_2 . In this section we will address two problems:

1. determining the wire tensions as functions of ρ_1, ρ_2 only
2. determining the region \mathcal{W} in the joint space such that $|\tau_1|, |\tau_2| \leq \tau_{max}$, where τ_{max} is a fixed threshold

For point 1 we note that the two first equations of (5) are linear in x_g, y_g . Solving this linear system and reporting the result in the last equation of (5) and in the 2 equations (2) leads to a system of 3 equations in θ, τ_1, τ_2 . This system may be converted into an algebraic system by using the Weierstrass substitution $T = \tan(\theta/2)$. Taking the resultant with respect to T of each pair of equations leads to two polynomials P_1, P_2 in τ_1, τ_2 , which have degree (6,6). For a given robot geometry the resultant of P_1, P_2 in τ_2 factor out in two polynomials of degree 12 and 20 in τ_1 , only the former one leading to valid values for τ_1 . Solving this polynomial and back substituting its roots in P_1, P_2 allow to calculate τ_2 , which complete the static analysis in the joint space.

For point 2 checking if, for a given mass of the platform, the value of the wire tensions are lower than the breaking point is clearly of interest. If only joint control

is use we are interested in determining the location of the points such that one of the wire tension is equal to its allowed maximum τ_{max} in the joint space ρ_1, ρ_2 .

Assume that we set $\tau_1 = \tau_{max}$; equations (3, 2) become a system of 5 equations in the unknowns x_g, y_g, θ, τ_2 . The first equation of (3) is used to determine τ_2 , while the difference between the 2 equations (2) is linear in x_g and is used to determine x_g . The second equation of (3) is linear in y_g : after solving it remains 2 equations (the third equation of (3) and one of the equations (2), that are only function of θ . If we define $T = \tan(\theta/2)$ the first equation may be written as the product of 3 polynomials $A \times B(T, \rho_1, \rho_2) \times C(T, \rho_1, \rho_2)$ of degree 2, 2, 4 in T , the polynomial B having only terms in ρ_1^2 or ρ_2^2 , while C is a 3rd order polynomial in ρ_1 and includes only terms with ρ_2^2 . The second equation may be written as $A \times D(T, \rho_1, \rho_2)$ where D is a sixth order polynomial in T and in ρ_1 , while it includes only ρ_2^4, ρ_2^2 terms. The common term A cancels when both wires are parallel, a case we have excluded. and consequently both equations will cancel either when the resultant of B, D or the resultant of C, D is equal to 0. The resultant of B, D factors out in a polynomial of degree 6 in ρ_1 and includes only ρ_2^4, ρ_2^2 terms. The resultant of C, D is too large to be obtained when the geometrical parameters of the robot are kept symbolic but it may be easily obtained for a given geometry and leads to a polynomial of degree 16 in ρ_1 and 12 in ρ_2 with a total degree 16.

To determine the region \mathcal{W} of the $\rho_1 - \rho_2$ joint space where we have $\tau_1 \leq \tau_{max}$ and $\tau_2 \leq \tau_{max}$ we have to plot the above curves for the two cases $\tau_1 = \tau_{max}$ and $\tau_2 = \tau_{max}$. These curves will be splitted in arcs whose start and end extremities are points such that either $\tau_1 = \tau_2 = \tau_{max}$ or $\tau_1 \leq 0$ or $\tau_2 \leq 0$ (the calculation in the joint space in the two later case being presented in section 5). Classically the border of \mathcal{W} will be obtained as a set of such arcs, which are determined by checking the constraints for the mid-point of the arcs, using a method that is similar to the one used for determining the workspace of a parallel robot [4].

We consider the test robot and we choose $\tau_{max} = 2\mathcal{F}$. Figure 3 shows the curves with the following notation: a curve denoted $\tau_i j$ is such that $\tau_i = \tau_{max}$ and a curve denoted v_i corresponds to the case where wire i supports all the load.

Consider the case where we have $\rho_1 = 40$. Setting $\tau_1 = \tau_{max}$ leads to 4 solutions $U_j = (\rho_2, \tau_2, x_g, y_g)$ with $U_1 = (42.96, 2.095, 49.7146, -6.66)$, $U_2 = (83.87, 1.989, 28.548, -8.8)$, $U_3 = (115.52, -1.517, -20.134, -23.017)$, $U_4 = (151.688, -1.4219, -35.554, -34.846)$. These points correspond to the intersection of the line $\rho_1 = 40$ with the arcs of curve denoted $\tau_{10}, \tau_{13}, \tau_{13}, \tau_{12}$. It may be noted that for points U_3, U_4 we have $\tau_2 < 0$: this is quite normal as these points are over the line v_1 . We notice also that for point U_1 we have $\tau_2 > 2$. If we now plot the 4 solutions (figure 4) we note that the solution U_2 corresponds to the unstable case where G lies over the point B_1, B_2 and, as expected, solutions U_3, U_4 lies on the left side of the y axis which is the limit in which wire 1 supports the whole load while wire 2 is slack. Hence none of these point may belong to the border of \mathcal{W} . If we consider the case $\tau_2 = \tau_{max}$ we get also 4 solutions (not represented in the figure) $V_j = (\rho_2, \tau_1, x_g, y_g)$ with $V_1 = (43.22, 1.905, 49.629, -7.192)$, $V_2 = (83.834, 2.01, 28.568, -8.733)$, $V_3 = (116.067, -2.262, -25.997, 14.647)$, $V_4 = (153.893365, -2.337226, -42.997, 25.872)$. For solutions V_3, V_4 we have $\tau_1 < 0$, while for V_2 we have $\tau_1 > \tau_{max}$ and a further analysis shows that

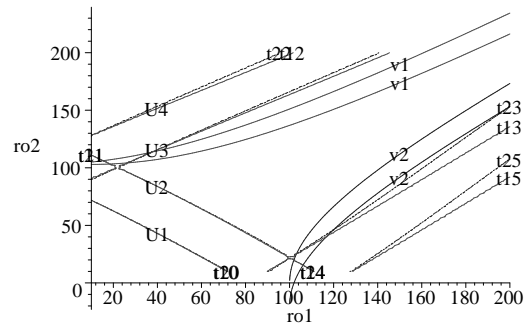


Fig. 3 The curves that appear in the calculation of the region in the $\rho_1 - \rho_2$ space for which $|\tau_1|, |\tau_2| \leq \tau_{max}$

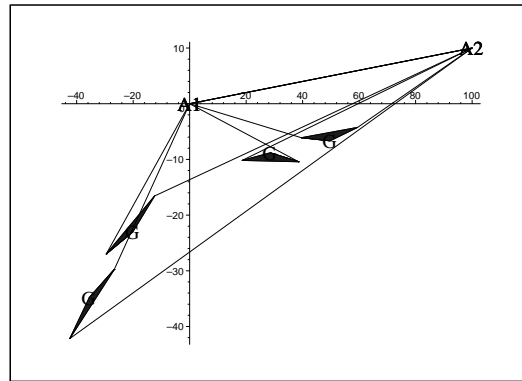


Fig. 4 The poses of the solutions obtained for $\rho_1 = 40$

this solution is also unstable. Hence the only valid solution is U_1 which is a point of the border of \mathcal{W} . A more complete analysis, that cannot be presented here for lack of space, shows that the region \mathcal{W} has as border the curve v_1 , v_2 , one arc of the curve t_{10} and one arc of the curve t_{20} .

5 Singularities

Wire-driven parallel robot have the same singularity than parallel robots with rigid legs (provided that the wire tensions are positive). In the 2-2 case this singularity will be obtained if the line A_1B_1, A_2B_2 are colinear. But this situation cannot occur for a crane as the mechanical equilibrium cannot be satisfied (the equilibrium along

the \mathbf{x} axis imposes $\tau_1 = -\tau_2$ and therefore the vertical force resulting from the wire tension is 0 and therefore cannot balance the weight of the platform).

But another type of singularity has to be considered namely when a wire tension cancels, as in that case we loose control of one d.o.f. For the 2-2 this happens when G, A_1, B_1 (or G, A_2, B_2) lies on the same vertical line. If we assume that only wire 1 is under tension we get $x_g = 0, x_1 = 0$ from which we get $\tan \theta = x_{b_i}/y_{b_i}$ while y_g has an arbitrary negative value. The minimal length of wire 2 may then be computed for a given y_g with equation (2). However it may be of interest to get the singularity condition in the joint space ρ_1, ρ_2 . If d_1 is the distance between G and B_1 we have $y_g = -\rho_1 \pm d_1$ Substituting this value in (2) leads to

$$\rho_2^2 \geq \left(\frac{y_{b_1} x_{b_2} - x_{b_1} y_{b_2}}{d_1} - x_{a_2} \right)^2 + \left(-\rho_1 \pm d_1 + \frac{x_{b_1} x_{b_2} + y_{b_1} y_{b_2}}{d_1} - y_{a_2} \right)^2 \quad (8)$$

which are the singularity conditions in the joint space. Another singularity condition can be obtained in the same way if wire 2 only is under tension.

6 Conclusion

In spite of its apparent simplicity the kinematics of the 2-2 robot is quite complex. This paper has addressed not so well known kinematics issues that may be of interest for the robot control either in the operational or in the joint space. The next step will then to extend the concepts proposed in this paper to spatial wire robots with 3 to 6 wires. This research has received funding from the European Community's Seventh Framework Program under grant agreement NMP2-SL-2011-285404 (CABLEBOT).

References

- [1] Bosscher, P., Ebert-Uphoff, I.: Wrench-based analysis of cable-driven robots. In: IEEE Int. Conf. on Robotics and Automation, pp. 4950–4955. New Orleans (April, 28-30, 2004)
- [2] Carricato, M., Merlet, J.P.: Stability analysis of underconstrained cable-driven parallel robots. IEEE Trans. on Robotics **29**(1), 288–296 (2013)
- [3] Carricato, M., Merlet, J.P.: Geometrico-static analysis of under-constrained cable-driven parallel robot. In: ARK, pp. 309–320. Piran (June 28- July 1, 2010)
- [4] Gosselin, C.: Determination of the workspace of 6-dof parallel manipulators. ASME J. of Mechanical Design **112**(3), 331–336 (September 1990)
- [5] Michael, N., Fink, J., Kumar, V.: Cooperative manipulation and transportation with aerial robots. In: Robotics: Science and Systems. Seattle (June 2009)